DETERMINATION OF THE MODEL COMPLEXITY LEVEL REQUIRED TO PREDICT THE CURE-INDUCED DEFORMATIONS IN THERMOSET-BASED COMPOSITE PARTS

A. Parmentier[a*], B. Wucher[a], D. Dumas[a]

[a]*Cenaero ASBL, Centre de recherche en aéronautique, Bâtiment Eole, Rue des Frères Wright 29, B-6041 Gosselies, Belgium, web page: http://www.cenaero.be*
**antoine.parmentier@cenaero.be*

Keywords: Composite, Simulation, Cure, Spring-in

Abstract
Composite parts used in aerospace structures become more and more complex. Understanding the mechanisms involved in the appearance of cure-induced deformations is therefore a key point in order to predict these deformations and to avoid the costly trial-and-error or empirical approaches currently used in mould design. One of the main challenges behind an accurate prediction of the residual stresses and deformations is the use of a model complexity level suited to the problem being studied. The present study aims at determining the numerical model complexity level allowing to predict the cure-induced deformations with sufficient accuracy and with reduced computational cost at the same time. Results show that a minimum effort in the model complexity level already give a robust model, able to predict the spring-in of simple geometries of various specifications: manufacturing process, stacking sequence, materials, cure temperature.

1. Introduction

Composite parts used in aerospace structures become more and more complex. Understanding the mechanisms involved in the appearance of cure-induced deformations is therefore a key point in order to predict these deformations and to avoid the costly trial-and-error or empirical approaches currently used in mould design. The deformations appear when curing thermoset-based composite materials, as the resin transforms from the liquid to the solid state. During this change of state, the part deforms due to thermal expansion and chemical shrinkage of the resin. In the case of open-mould processes such as autoclave or vacuum infusion, the contact conditions with the mould as well as the pressure exerted on the part prevent these deformations from developing freely and internal stresses build up. Upon demoulding, part of the internal stresses is released, resulting in the appearance of distortions. One of the main challenges behind an accurate prediction of the residual stresses and deformations is the use of a model complexity level suited to the problem being studied.

The present study aims at determining the numerical model complexity level allowing to predict the cure-induced deformations with sufficient accuracy and with reduced computational cost at the same time. Three boundary conditions of different complexity were tested: “freestanding cure”, “fully constrained cure” followed by a demoulding step and

"autoclave" conditions (applied pressure on top of the part and the mould is modelled as a rigid part).

The spring-in angle Δθ characterizes the difference between the nominal geometry or mould geometry and the cured geometry for angle brackets as illustrated on Figure 1.

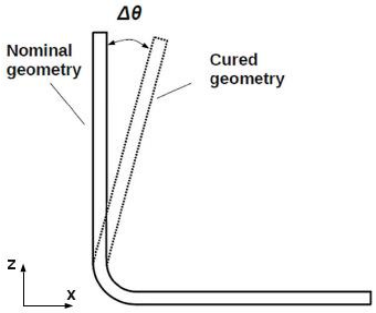

Figure 1. Definition of the spring-in angle.

2. Method

2.1. Experimental

In order to evaluate the accuracy of the models tested, an experimental study was performed. Parts of different shapes and manufacturing conditions were made to evaluate the limits of the model in term of manufacturing conditions and geometrical complexity. The spring-in angle of parts is studied through angle brackets in L and Z shapes made respectively on epoxy resin and invar tools. Unlike Invar which presents a low thermal expansion coefficient (CTE), the epoxy resin of the tool exhibits an important CTE and the deformation due to the interaction with the mould is not negligible as previously shown by other researchers [1, 2].

The L-shaped parts were manufactured using the Vacuum Assisted Resin Transfer Moulding (VARTM) process on an epoxy resin male mould. The angle brackets are 280 mm long with 100 mm long flanges. The parts are produced by vacuum infusion with a Saertex quasi UD glass fabric (90% of the fibres in the warp direction) and the Araldite LY5052/Hardener HY5052 epoxy resin system produced by Huntsman. The stacking sequence is the same for all the parts: the fibres are oriented in the direction perpendicular to the y-axis on Figure 1, which is the 0° direction. The parts were cured long enough to reach their maximal degree of cure and then cooled to room temperature. Each configuration was manufactured at least 5 times in order to smooth the differences between experimental conditions. The influence of the cure temperature and number of plies on the spring-in angle was tested experimentally: different parts with 50 or 70°C cure temperature and various thicknesses, 6 or 12 plies, were manufactured.

Z-shaped parts are made of a plain weave prepreg of carbon fibres AS4/8552 produced by Hexcel and cured within autoclave. The male angle of the tool is referred as A1 in the following while A2 is the female angle. The Z-shaped parts are 150mm long with 100mm long flanges. The stacking sequence first observed is composed of 15 plies: [±45°/0-90°]4s. Four specimens were manufactured. The cure cycle applied is a cycle used by aeronautic companies and applied while curing secondary structures. To evaluate the robustness of the model, three additional parts with varying stacking sequences and materials were manufactured:

- [(±45/0-90)2/±45/±45/0-90/±45]: asymmetrical stacking sequence of plain weave prepreg of carbon fibres AS4/8552;
- [GFRP/(±45°/0-90°)4]s: symmetrical layup, with one ply of 8H satin weave prepreg of E-glass fibres 7781/8552 resin on each surface;
- [GFRP/(±45°/0-90°)4s]: symmetrical layup of CFRP, with one ply of glass fibres prepreg on the tool side surface of the part.

Plies of glass fibres prepreg are commonly used in aeronautic applications to prevent corrosion when there is contact between aluminium and carbon fibres.

The distortions of the parts are measured using a Nikon MMDx100 laser scanner mounted on a 7-axis Metrology-grade MCA II arm. The declared accuracy is 54 µm which leads to an incertitude of 0.1° on the spring-in angle measured.

2.2. Numerical

The numerical prediction methodology that is used consists in performing coupled chemical-mechanical Finite Elements (FE) calculations using ABAQUS with the help of user material subroutines. The transient thermal problem is not solved: the temperature is considered to be uniform throughout the part, because of its low thickness. The details of the model follow the approach suggested by Svanberg and Holmberg [3] which considers a simplified linear viscoelastic behaviour of the material where time-temperature-degree of cure superposition is applied. Three of the main assumptions made are: (i) the stresses and strains are assumed to be zero until gelation, (ii) both thermal expansion and chemical shrinkage are assumed to be linear within each material state, and, (iii) the material properties are kept constant for each relevant state, rubbery or glassy, of the resin. The transition from the rubbery to glassy state happens when the resin temperature reaches its glass transition temperature Tg which is assumed to depend only on the degree of cure X. The model used to predict the glass transition temperature Tg as a function of the degree of cure X and the kinetic model are those used in [4] for the LY5052 resin and in [5] for the 8552 resin.

Even with the assumptions made, 31 material properties are needed in total for both states, rubbery and glassy. The material properties used for numerical simulations are presented in Table 1. The references of the properties taken from the literature are specified in the Table below. The missing properties of the carbon fabric prepreg have been determined using the Classical Laminate Theory from the properties of the UD prepreg 8552/AS4 found in the literature [6] and micromechanics calculations. The properties of the glass fabric prepreg have been determined using micromechanics calculations from the properties of the components: 8552 resin [6] and E-glass fibres [7]. Chemical shrinkage coefficients were calculated using micromechanics calculations and the equation β(X) given in [5].

Different boundary conditions are applied:

- Freestanding-cure (NC) which means that the part is free to deform. The rigid body motions are blocked to prevent the part to move;
- Fully-constrained cure (FC): all the nodes are blocked during cure. A demoulding step is performed to release the nodes and account of the deformation;
- Autoclave conditions (Autoclave): the autoclave pressure is applied on top of the part and a rigid mould is modeled with a frictionless contact condition between the part and the mould. Modeling the mould as a rigid part makes sense as the tool used in autoclave is made of Invar which exhibits a low coefficient of thermal expansion. The

objective is to have a boundary condition that is closer to the experimental setup: the autoclave keeps the part against the mould and the mould prevents the angle to close during cure.

	Carbon fabric prepreg 8552/AS4		**Glass fabric prepreg 8552/7781**		**Quasi UD glass fabric Saertex/LY5052**	
	Rubbery	Glassy	Rubbery	Glassy	Rubbery	Glassy
E1 [MPa]	66190	68000 [8]	18030	26080	37200	38600
E2 [MPa]	66190	68000 [8]	18030	26080	1000	7000
E3 [MPa]	165 [6]	10000 [8]	132.53 [6]	13438	1000	7000
υ21	0.001	0.220 [8]	0.003	0.162	9.7E-04	0.054
υ31	0.002	0.072 [8]	0.004	0.182	9.7E-04	0.054
υ23	0.833	0.490 [8]	0.532	0.353	0.980	0.520
G12 [MPa]	44.3	5000 [8]	44.2	4955.6	30	2600
G13 [MPa]	42.9	4500 [8]	44.2	4955.6	30	2600
G23 [MPa]	42.9	4500 [8]	44.2	4955.6	30	2300
α1 [1/°C]	-7.11E-07	2.5E-06	5.6E-06	1.57E-05	5E-06	7.2E-06
α2 [1/°C]	-7.11E-07	2.5E-06	5.6E-06	1.57E-05	136E-06	50.7E-06
α3 [1/°C]	0.0002 [5]	62.5E-06 [5]	0.0002	7.02E-05	136E-06	50.7E-06
β1	9.3E-04*β(X)	5.3E-02*β(X)	3.4E-03*β(X)	0.20*β(X)	-9E-05	-8E-04
β2	9.3E-04*β(X)	5.3E-02*β(X)	3.4E-03*β(X)	0.20*β(X)	-1.8-02	-1.6E-02
β3	β(X) [5]	β(X) [5]	1.17*β(X)	1.138	-1.8-02	-1.6E-02

Table 1. Properties of the different materials used in the simulations. Directions 1 and 2 stand for the fibres direction of the fabric prepreg. Direction 1 stands for the fibres direction of the UD. α and β stand for the thermal expansion coefficient and the chemical shrinkage, respectively.

3. Results and discussion

3.1. Vacuum infusion – L-shaped parts

The numerical predictions are compared to the measured spring-in, Figure 2, for the specimens produced by vacuum infusion. The error bars present the standard deviation of the measurements. Attention should be paid while interpreting the spring-in value for the "6 plies, 50°C" case because of the important standard deviation observed (±0.37°). In all cases, the measured spring-in stands between the predictions. This was expected as the two boundary conditions, "freestanding" and "fully-constrained" cure, are extremes cases. In reality, the part is not totally free to deform because of the 1 bar pressure applied by the vacuum bag and the presence of the mould, but is not fully constrained either.

The simulations performed in this study, both "freestanding" and "fully-constrained" cure, are able to predict the behaviour observed experimentally in term of cure temperature and are in agreement with other studies [9]: a higher cure temperature increases the spring-in angle since both thermal strains and degree of cure are more important when the cure temperature is higher. However, the simulation results are not significantly influenced by the thickness of the parts while experimental results showed a reduction of the spring-in angle for thicker parts.

Experimental results are in accordance with observations made in other studies and reported in [1, 10, 11]. These studies have shown the role of the interaction with the mould which has not been modelled here.

The spring-in angle seems to be underestimated by the prediction. This can be explained by the gradient of fibre volume fraction in the thickness of the part at the angle. On a male angle, the contact zone between the part and the tool is subjected to a higher pressure. The resin is swept and the fibre volume fraction increases locally, closed to the mould. This tends to reduce the spring-in compared to the simulation which considers a constant fibre volume fraction in the thickness. The influence of the fibre volume fraction gradient on the spring-in has already been identified in [10].

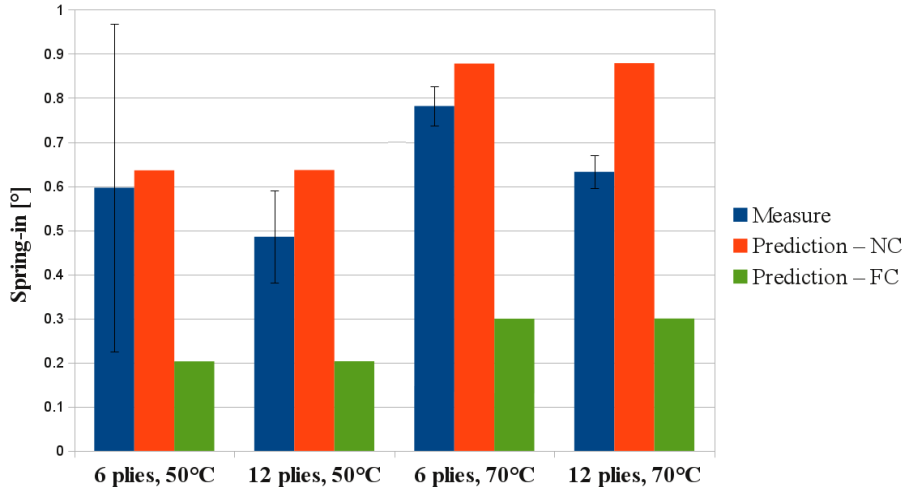

Figure 2. Comparison between predicted and measured spring-in on L-shaped parts made by VARTM.

3.2. Autoclave – Z-shaped parts

The numerical predictions are compared to the measured spring-in for the specimens with a symmetrical stacking sequence on Figure 3. The error bars take into account the measurement uncertainty (0.1°) and the standard deviation observed by averaging all the values of all the sections of the four parts manufactured. Compared to the L angle brackets, a third boundary condition was tested, closer to the autoclave conditions as described in section 2.2. A pressure of 7 bars is applied at the surface of the part during the cure cycle. The mould is modelled as a rigid part which makes more sense in that case compared to the L-shaped parts, as the real mould is made of Invar (which presents a low CTE), and not in epoxy resin (which exhibits a significant CTE).

As previously observed on the parts made by vacuum infusion, the measured spring-in stands between the predictions “NC” and “FC” except the measure of the spring-in on A2 for the 15 plies of CFRP case (Figure 3). A closer look at the specimens manufactured with that stacking sequence showed that much more resin is present in that angle. During cure, the resin flowed and sat in the female angle of the mould (A2). This can explain the higher spring-in angle observed in that angle due to the resin shrinkage, which is more important, and supports the role of the fibre volume fraction gradient explained in section 3.1. The prediction made on the angle A1, which is the male angle of the tool, is slightly overestimated as observed on the L-shaped parts. The potential influence of the fibre volume fraction has been explained in section 3.1. The comparison (Figure 3) shows that the predictions made using the

freestanding-cure boundary conditions (NC) give the best results. The use of a more complex boundary condition, "Autoclave", is heavier in computational time and does not bring any improvement.

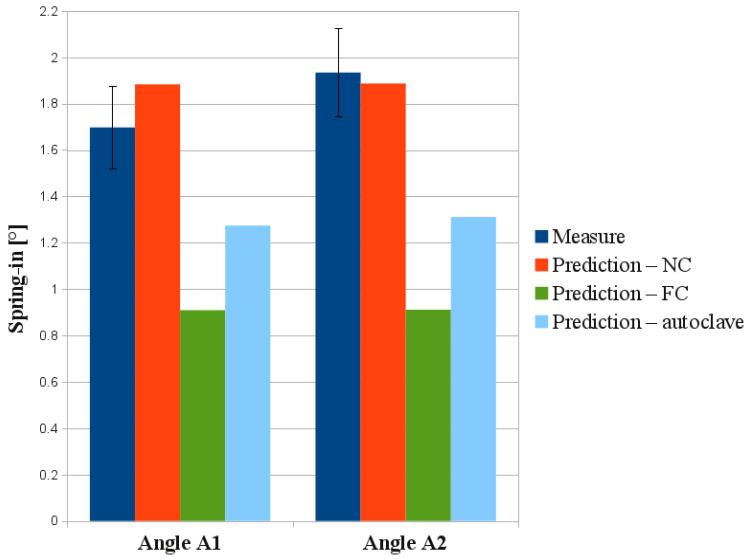

Figure 3. Comparison between predicted and measured spring-in on Z-shaped parts with a symmetrical stacking sequence: [±45/0-90]4s cured within autoclave

The model has also been evaluated on an asymmetrical stacking sequence. The experimental measurements are compared to the predictions on Figure 4. As observed on a symmetrical layup, the "Autoclave" prediction stands between the two extreme cases, "NC" and "FC". The spring-in predicted using the freestanding-cure boundary conditions (NC) stands within the uncertainties on the experimental measures.

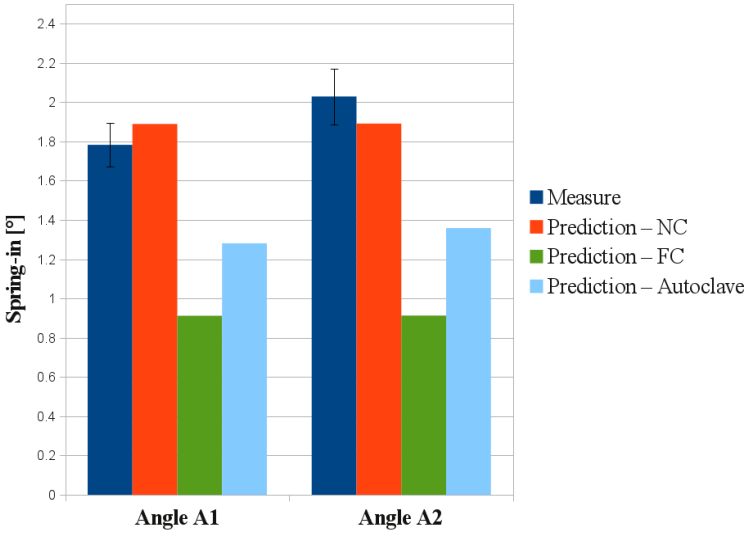

Figure 4. Comparison between predicted and measured spring-in on Z-shaped parts with an asymmetrical stacking sequence: [(±45/0-90)2/±45/±45/0-90/±45] cured within autoclave.

The experimental influence of glass fibres plies is shown in Figure 5a. Adding one ply of GFRP on both surfaces does not bring any significant change in the deformation. However, adding one GFRP ply on one surface only makes the stacking sequence asymmetrical and seems to be enough to change the deformation. The spring-in increases on A1: the ply is lain

inside the fillet radius. The GFRP fibres cannot withstand the chemical shrinkage as the CFRP fibres do, so the ply acts like a layer of resin, shrinks and increases the spring-in angle. On A2, the GFRP ply is laid outside the fillet radius. The experimental results (Figure 5a) can be compared to predictions on Figure 5b. The NC boundary conditions have been chosen as they show the best prediction results. The influence of the GFRP plies observed experimentally is reproduced by numerical simulations. The predictions are close to the measurements: in all cases but one (A2 of [GFRP/(±45°/0-90°)4s]) the predicted value stands within the measurement uncertainty.

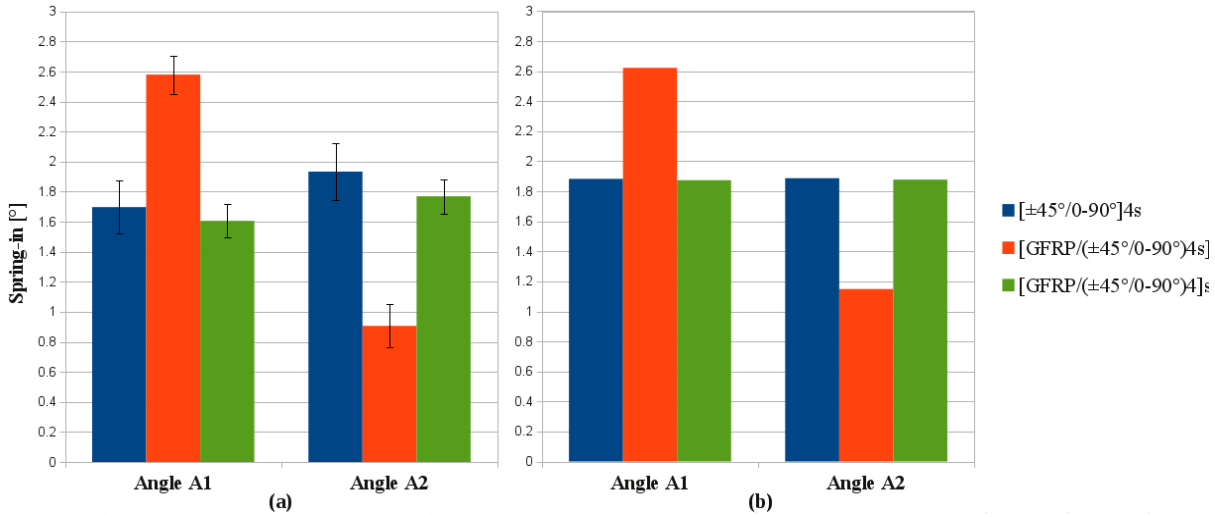

Figure 5. Influence of GFRP plies, both (a) experimental and (b) numerical, on the spring-in angle.

4. Conclusion

The model established in this study has been evaluated by comparison with experimental measurements taken on specimens of various features: different manufacturing processes, cure temperatures, thicknesses, stacking sequences and materials. The predicted spring-in has been close to the experiments for most of the configurations. For all the parts made by vacuum infusion or within autoclave, the predictions using freestanding-cure boundary conditions always give the best results. An attempt has been made by applying boundary conditions closer to the autoclave conditions without any improvement in the results, but with heavier calculations.

The predictions of the spring-in of the parts made within autoclave are closer to the experimental measurements. This can be explained by two different phenomena:

- The fibre volume fraction is more difficult to control using vacuum infusion than prepregs in autoclave, where the fibre volume fraction is expected to be more uniform. As explained in section 4 and showed experimentally on the parts where a resin heap has been observed, the gradient of fibre volume fraction in the fillet radius can influence the spring-in angle [10];
- Another difference is that the parts made by vacuum infusion have been manufactured on an epoxy resin mould which presents a higher CTE than composites, which can influence the deformation [1, 2, 10, 11]. Modelling the epoxy resin mould should help to improve the numerical results obtained on L-shaped parts.

The robustness of the model is difficult to validate on parts produced by vacuum infusion due to the high variability in the quality of parts. Taking into account the points listed above in the

numerical simulation should help improving the predictions. However, with a more controlled manufacturing process as the autoclave process, the predictions are close to the experimental data. Different stacking sequences, symmetrical and asymmetrical, and materials, CFRP with/without GFRP, have been studied with no significant degradation of the predictions, which show the robustness of the model. An important uncertainty comes from the materials properties which have been found in the literature. The missing properties were determined using micromechanical equations and composite laminate theory. A sensitivity analysis of the properties values on the deformation will be performed in future work in order to highlight the properties to be characterized accurately to ensure the reliability of the results.

Simulations with little effort and light computational cost already give fairly good results on simple geometries. As a further step, the model will be validated on a more complex part.

References

[1] G. Fernlund and C. Albert. Spring-in and warpage of angled composite laminates. *Composites Science and Technology*, 62(14):1895-1912, 2002.

[2] G. Fernlund, G. Twigg and A. Poursartip. Tool-part interaction in composite processing Part 1: experimental investigation and analytical model. *Composites Part A: Applied Science and Manufacturing*, 35(1):121-133, 2004.

[3] J.M. Svanberg and J.A. Holmberg. Predictions of the shape distortions Part I. FE-implementation of a path dependent constitutive model. *Composites Part A: Applied Science and Manufacturing*, 35(6): 711-772, 2004.

[4] J.M. Svanberg. Shape distortion of non-isothermally cured composite angle bracket. *Plastics, Rubber and Composites*, 31(9):398-404, 2002.

[5] N. Ersoy and al. Development of spring-in angle during cure of a thermosetting composite. *Composites Part A: Applied Science and Manufacturing*, 36(12): 1700-1706, 2005

[6] N. Ersoy and al. Development of the properties of a carbon fibre reinforced thermosetting composite through cure. *Composites Part A: Applied Science and Manufacturing*, 41(3):401-409, 2010.

[7] D. Gay. *Matériaux Composites*, Hermes Science Publications, Paris, 2005.

[8] J.A. Artero and al. On the influence of filling level in CFRP aircraft fuel tank subjected to high velocity impacts. *Composite Structures*, 107:570-577, 2014.

[9] J.M. Svanberg and J.A. Holmberg. An experimental investigation on mechanisms for manufacturing induced shape distortions in homogeneous and balanced laminates. *Composites Part A: Applied Science and Manufacturing*, 32(6): 827-838, 2001.

[10] D.A. Darrow and L.V. Smith. Isolating components of processing induced warpage in laminated composites. *Journal of Composite Materials*, 36(21): 2407-2419, 2002.

[11] M.R. Wisnom, K.D. Potter and N. Ersoy. Shear-lag analysis of the effect of the thickness on spring-in of curved composites. *Journal of Composite Materials*, 41(11): 1311-1324, 2007.